Reviews on Advanced Materials and Technologies, 2026, vol. 8, no. 2, pp. 117–124
DOI: 10.17586/2687-0568-2026-8-2-117-124

Performance Evaluation of Fiber-Converged Free-Space Optical Systems in Emulated Atmospheric Turbulence

D.I. Balovnev *, **D.S. Shiryaev**, **I.S. Polukhin**, **E.S. Kolodeznyi**

Institute of Advanced Data Transfer Systems, ITMO University, Birzhevaya Line, 14, St. Petersburg, 199034, Russia

Article history

Received March 30, 2026
Received in revised form, May 29, 2026
Accepted June 19, 2026
Available online June 30, 2026

Abstract

Free-space optical (FSO) systems that interface directly with optical fibers offer enhanced flexibility and compatibility with modern fiber-optic transceivers, but their performance is strongly influenced by atmospheric turbulence and fiber-coupling efficiency. In this work, a custom-developed atmospheric chamber is presented for controlled and repeatable emulation of turbulence with real-time estimation of the refractive-index structure parameter. Using fiber-coupled FSO modules, the recorded optical power fluctuations were measured for single-mode (SMF) and multimode fiber (MMF) coupling under identical turbulence conditions spanning $C_n^2 \approx 10^{-16}$ to 10^{-11} $m^{-2/3}$. Experimental results show that strong turbulence causes severe power scintillations for SMF coupling (standard deviation ≈ 5.16 dB), while MMF coupling remains highly stable (standard deviation ≈ 0.08 dB). These findings demonstrate the strong resilience of MMF coupling to turbulence-induced wavefront distortions and validate the atmospheric chamber as an effective and repeatable platform for investigating turbulence effects in fiber-converged FSO systems, providing practical insights for system design and performance optimization.

Keywords: Free-space optics (FSO); Atmospheric turbulence; Fiber coupling

1. INTRODUCTION

Free-space optical (FSO) communication has attracted significant research interest due to its capability to provide high data rates, strong inherent security, and access to a large unlicensed bandwidth [1]. These features make FSO a promising solution for future broadband communication systems. In practical implementations, however, the realization of these advantages depends not only on channel conditions but also on the architectural design of the optical terminals and their degree of compatibility with fiber-optic technologies widely used in modern communication networks. Conventional FSO terminals rely on bulk optical components for beam reception, detection, and signal processing. While such systems can achieve high performance, they often lack flexibility and interoperability with commercially available fiber-optic components, such as standard transceivers and erbium-doped fiber amplifiers. In contrast, fiber-converged FSO systems employ optical fiber interfaces at both the transmitter and receiver, enabling seamless integration with existing fiber-optic infrastructure. This approach supports modular system architectures and has the potential to reduce overall cost and complexity [2]. Nevertheless, the use of fiber interfaces introduces additional performance constraints, as overall system performance becomes strongly dependent on the efficiency of coupling the received free-space beam into an optical fiber.

Among the various impairments affecting FSO propagation, atmospheric turbulence is one of the most critical. Turbulence arises from random fluctuations in air temperature and pressure, which lead to spatial and temporal variations in the refractive index along the propagation path. These inhomogeneities distort the optical wavefront and give rise to beam wandering, beam spreading, and scintillation [3]. In fiber-coupled FSO systems, such effects directly reduce coupling efficiency at the receiver and result in time-varying power fading. When single-mode fiber

* Corresponding author: D.I. Balovnev, e-mail: dibalovnev@itmo.ru

is employed, even small wavefront distortions can cause substantial coupling losses due to stringent mode-matching requirements, leading to significant performance degradation. To mitigate turbulence-induced coupling losses, alternative receiver strategies based on few-mode or multimode fibers have been proposed [4].

Fibers with larger core diameters and numerical apertures are inherently more tolerant to beam wander and wavefront distortions, as distorted optical fields can be coupled into higher-order spatial modes. Several studies have reported improved coupling efficiency and reduced power fading when multimode fiber (MMF) is used instead of single-mode fiber (SMF) under turbulent conditions [5,6]. Nonetheless, MMF coupling may introduce additional impairments such as modal dispersion and has limited compatibility with standard single-mode fiber networks. Consequently, a clear experimental understanding of the trade-offs between SMF and MMF coupling under well-defined turbulence conditions is essential for the design of fiber-converged FSO systems.

Recent studies on turbulence-induced fiber-coupling degradation rely on analytical modeling, numerical simulations [7], or outdoor field experiments [8]. While outdoor measurements capture realistic propagation conditions, they are inherently difficult to control and reproduce, and the turbulence strength is often only indirectly estimated. Laboratory-based turbulence emulation platforms offer a complementary approach by enabling controlled and repeatable experimentation. Atmospheric chambers that generate turbulence through controlled temperature gradients allow real-time monitoring of environmental parameters and systematic variation of turbulence strength.

In this work, we experimentally investigate the impact of atmospheric turbulence on fiber-converged FSO links using a custom-made atmospheric chamber designed to emulate different turbulence regimes in a controlled laboratory environment. Spatial temperature measurements along the optical path are used to estimate the refractive-index structure parameter C_n^2, providing quantitative characterization of turbulence strength. Using two fiber-coupled FSO modules, we record received optical power time series for both single-mode and multimode fiber coupling under varying turbulence conditions. Statistical analysis of the measured data is performed to compare power stability and fading characteristics for the two fiber types. The presented results contribute to a better understanding of turbulence-induced limitations in fiber-coupled FSO systems and provide practical insights for the design of flexible and cost-efficient FSO architectures based on fiber-optic components. Compared with previous studies based primarily on numerical modeling or outdoor measurements, the present work provides a controlled experimental investigation of turbulence-induced degradation in fiber-converged FSO systems using a custom-made atmospheric chamber with estimation of the refractive-index structure parameter. The main contribution of this study is the direct experimental comparison of single-mode and multimode fiber coupling under identical and repeatable turbulence conditions.

2. METHODS

2.1. Experimental setup

Atmospheric effects in the free-space optical channel were emulated using a dedicated laboratory-scale atmospheric chamber with overall dimensions of 2000 × 400 × 400 mm, as shown in Fig. 1. The chamber is constructed from optically transparent material and forms a closed volume with optical access windows at both ends, allowing the integration of optical components with apertures up to 2 inches. The chamber was designed to provide a controlled and

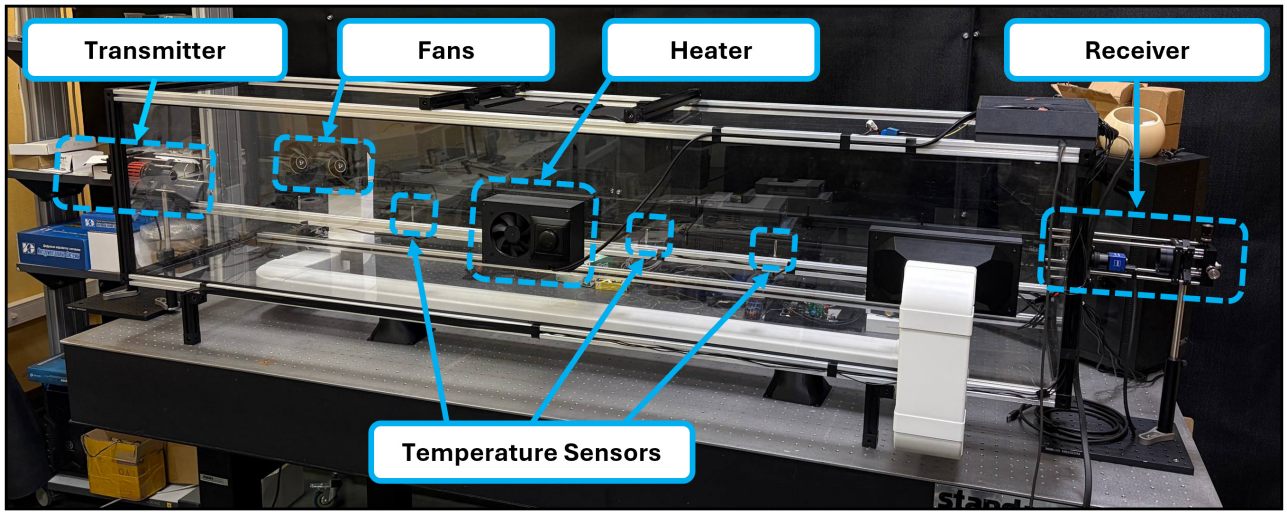

Fig. 1. Custom-made atmospheric chamber used to generate weak-to-strong atmospheric turbulence.

repeatable environment for generating atmospheric turbulence along the optical propagation path.

Six digital temperature sensors (DS18B20) were positioned along the beam axis at regular intervals of 150 mm to monitor spatial and temporal temperature variations. An adjustable heating element was installed in the central region of the chamber to generate localized thermal gradients and induce convective air motion. In addition, four fans, two on each side of the chamber, were used to control airflow along and across the optical path, enabling modulation of turbulence intensity. All active components were controlled using an ESP32 microcontroller, which also facilitated real-time acquisition of temperature data.

2.2. Turbulence characterization

The strength of atmospheric turbulence inside the chamber was quantified using the refractive-index structure parameter C_n^2, which is widely adopted as the standard metric for characterizing optical turbulence. The estimation of C_n^2 was based on direct temperature measurements obtained from spatially distributed sensors.

For statistically homogeneous and isotropic turbulence, the second-order temperature structure function is defined as:

$$D_T(L) = \left\langle (T_1 - T_2)^2 \right\rangle = C_T^2 L^{2/3}, \tag{1}$$

where T_1 and T_2 are temperatures measured at two locations separated by distance L, $\langle\ \rangle$ denotes ensemble averaging, and C_T^2 is the temperature structure parameter.

From this relation, the temperature structure parameter can be expressed as:

$$C_T^2 = \frac{D_T(L)}{L^{2/3}}. \tag{2}$$

In the present setup, L corresponds to the spacing between adjacent temperature sensors, and $D_T(L)$ was calculated from the measured temperature differences along the chamber axis.

The refractive-index structure parameter C_n^2 is related to the temperature structure parameter through:

$$C_n^2 = \left(A \frac{P}{T^2} \right)^2 C_T^2, \tag{3}$$

where P is the atmospheric pressure (in mbar), T is the absolute temperature (in Kelvin), and $A = 80 \times 10^{-6}$ K/mbar. Since the experiments were conducted at constant laboratory altitude, pressure variations were negligible and treated as constant.

2.3. Data acquisition and statistical analysis

A simplified schematic representation of the experimental setup is shown in Fig. 2. The experimental FSO link was established by placing two fiber-coupled collimators at opposite ends of the atmospheric chamber, serving as the transmitting and receiving optical terminals. A continuous-wave laser source (Yenista TUNICS T100S-HP) operating at a wavelength of 1550 nm and an output power of 0 dBm was coupled into the Tx collimator. At the receiver side, the Rx collimator was connected to either a SMF or a MMF, depending on the measurement configuration, and interfaced with an optical power meter. The received optical power was recorded as a time series at sampling rates between 10 and 1000 Hz to capture turbulence-induced power fluctuations. All measurements were conducted with fixed optical alignment to isolate the impact of atmospheric turbulence on fiber-coupling performance.

3. RESULTS AND DISCUSSION

Fig. 3a shows the temporal evolution of the temperature measured by six sensors distributed along the optical propagation path during the activation of the atmospheric cham-

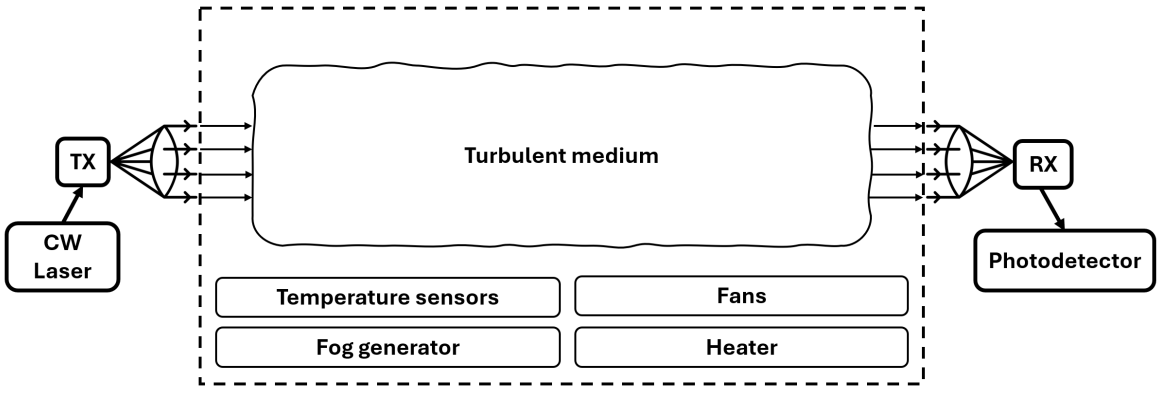

Fig. 2. Schematic representation of the experimental setup used for turbulence emulation and optical power measurements.

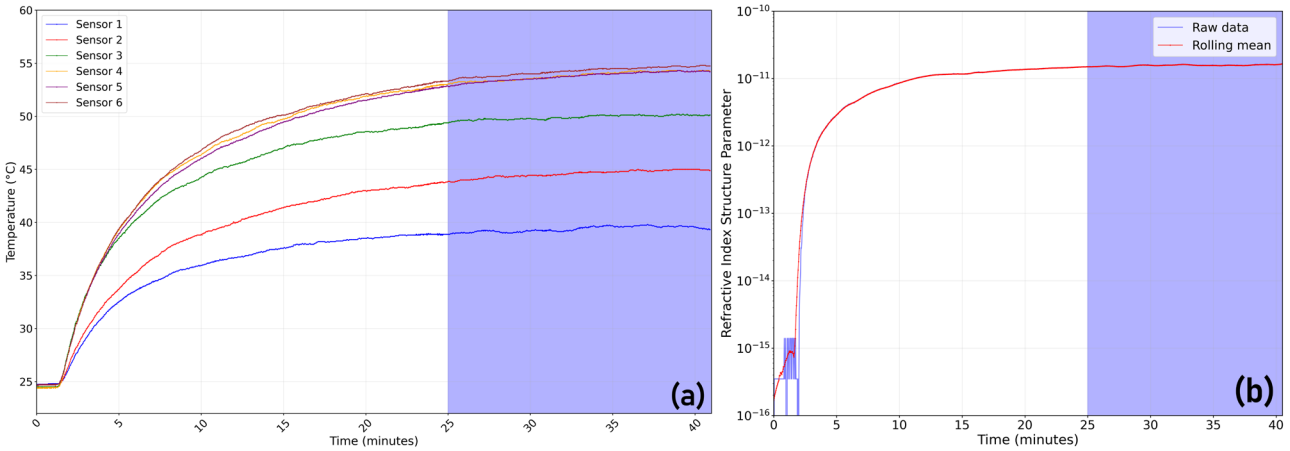

Fig. 3. Temporal evolution of (a) temperature and (b) refractive index structure parameter.

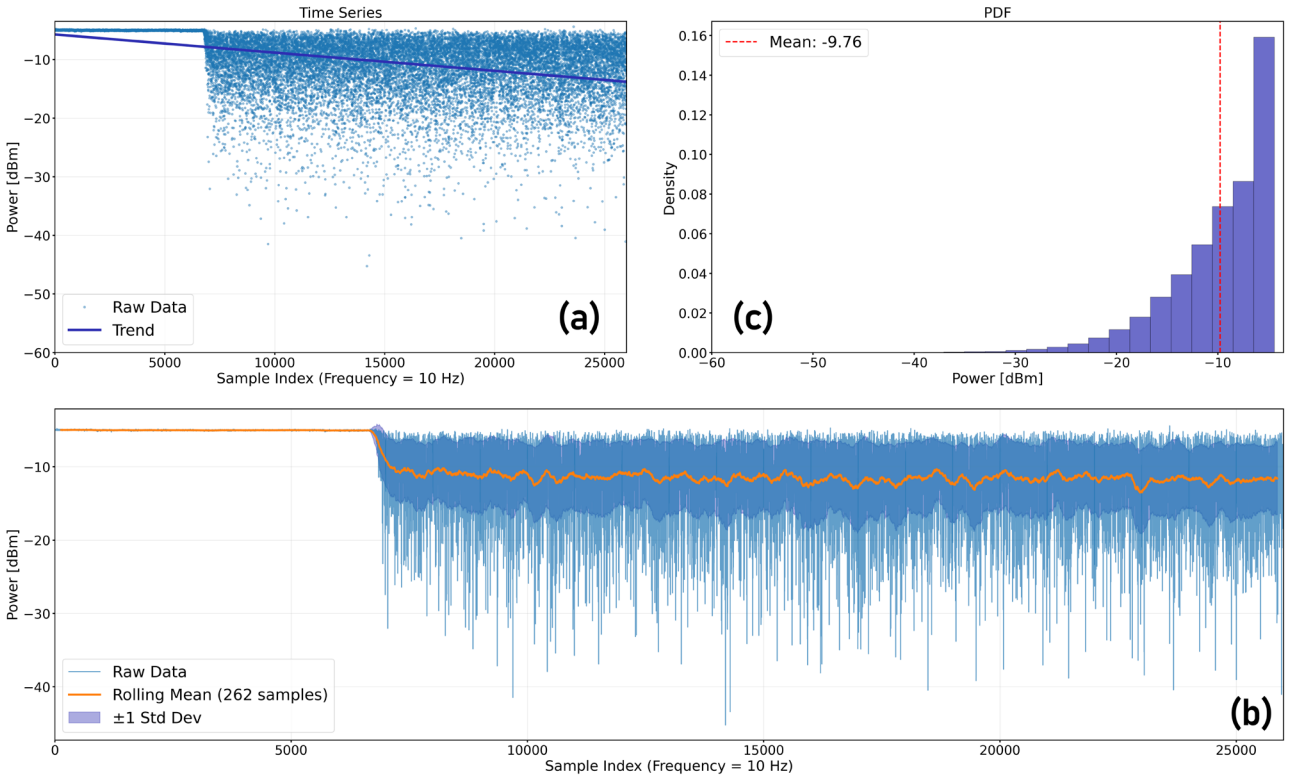

Fig. 4. (a,b) Optical power received under the influence of atmospheric turbulence during the experiment; (c) PDF of the measured data as a function of the power.

ber. At the beginning of the experiment, all sensors exhibited stable and nearly identical temperature values, indicating thermal equilibrium and negligible turbulence. Upon activation of the heating element and airflow control, temperature gradients gradually developed, leading to sustained non-uniform temperature fluctuations along the chamber length. The highlighted region in Fig. 3 corresponds to the period during which strong thermal gradients are maintained.

Using the recorded temperature data, the refractive-index structure parameter C_n^2 was calculated as a function of time according to Eqs. (1)–(3). The resulting C_n^2 evolution is presented in Fig. 3b. During the initial equilibrium phase, C_n^2 remains on the order of 10^{-16} $m^{-2/3}$, corresponding to a weak or nearly turbulence-free regime. As thermal gradients intensify, C_n^2 increases by several orders of magnitude and stabilizes around 10^{-11} $m^{-2/3}$ within the highlighted region. This value is characteristic of strong turbulence and remains relatively stable over time, demonstrating that the chamber can generate sustained and repeatable turbulent conditions suitable for controlled FSO experiments. The impact of turbulence on fiber coupling was first evaluated using a single-mode fiber at the receiver. Fig. 4 presents the received optical power as a function of time during the whole experiment.

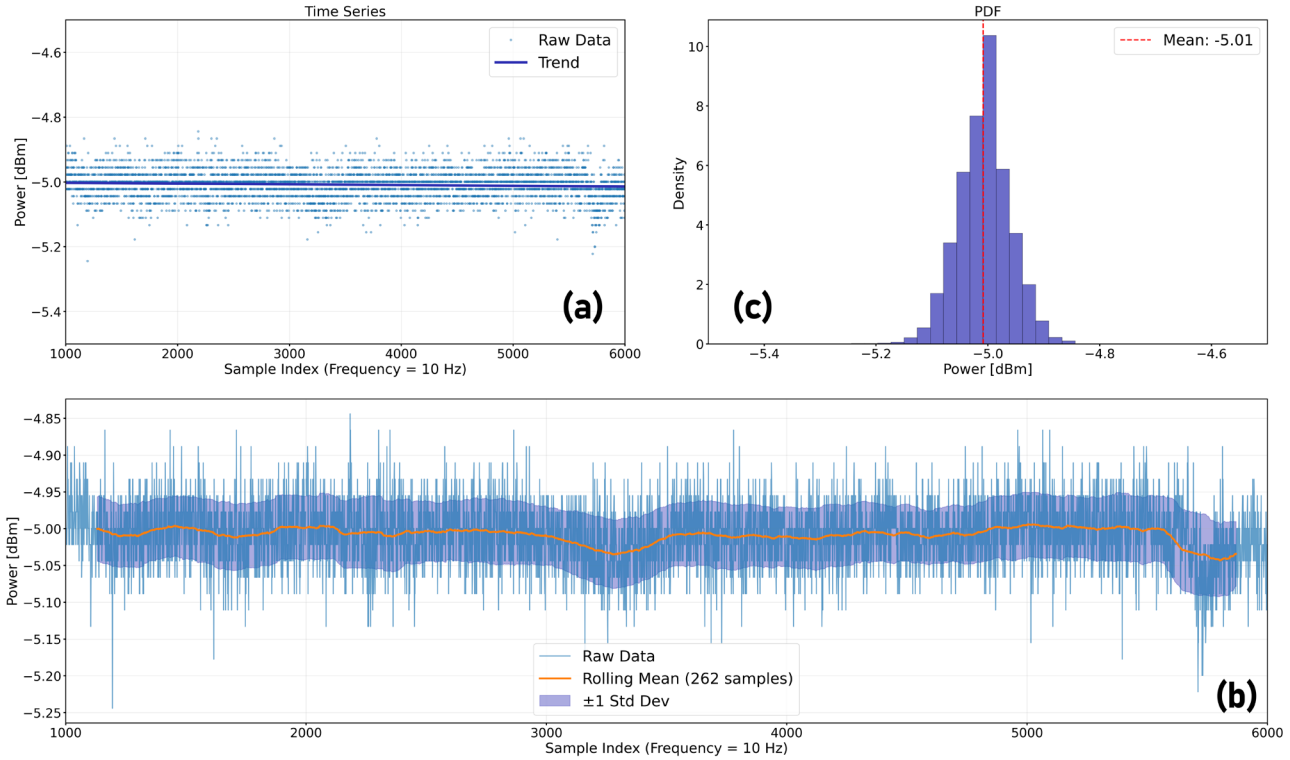

Fig. 5. (a,b) Optical power received (SMF) under weak turbulence conditions with $C_n^2 \approx 10^{-16}$ m$^{-2/3}$; (c) PDF of the measured data as a function of the power.

A clear transition is observed when turbulence generation begins: the initially stable power level rapidly evolves into pronounced temporal fluctuations. This behavior is consistent with turbulence-induced wavefront distortions that degrade mode matching between the received beam and the SMF. To quantify these effects, power data were analyzed separately for periods without turbulence and under strong turbulence. Fig. 5 shows the received power samples and the corresponding probability density function (PDF) for the weak turbulence regime ($C_n^2 \approx 10^{-16}$ m$^{-2/3}$).

The mean received power is −5.01 dBm, with a very low standard deviation of 0.045 dB and a dynamic range of 0.40 dB. The measured PDF closely follows a log-normal distribution, in agreement with classical turbulence theory and prior experimental studies, which predict log-normal irradiance statistics in weak or negligible turbulence conditions. In contrast, Fig. 6 shows the received power statistics for the SMF-coupled receiver under strong turbulence ($C_n^2 \approx 10^{-11}$ m$^{-2/3}$).

The mean received power drops significantly to −11.99 dBm, corresponding to an average coupling loss of nearly 7 dB relative to the non-turbulent case. At the same time, the standard deviation increases to 5.16 dB, and the dynamic range expands to 48.88 dB, indicating severe power fading. The PDF shifts toward lower power levels and is well described by a gamma–gamma distribution, which is widely accepted as an accurate model for irradiance fluctuations in strong turbulence regimes. These results clearly demonstrate high sensitivity of SMF coupling to atmospheric turbulence. To evaluate the effect of fiber type on turbulence resilience, the SMF at the receiver was replaced with a MMF, while all other experimental conditions were kept unchanged. Fig. 7 shows the received power statistics for MMF coupling under the same strong turbulence regime. Compared to the SMF case, the MMF-coupled system exhibits a markedly different behavior. The mean received power increases to −4.19 dBm, exceeding the SMF no-turbulence average. Moreover, the standard deviation is reduced to 0.0843 dB, and the dynamic range is limited to 0.67 dB. These values indicate a near-complete suppression of turbulence-induced power fading. This strong improvement can be attributed to the larger core diameter and numerical aperture of the MMF, which allow distorted wavefronts and beam wander components to be efficiently coupled into higher-order guided modes. As a result, the MMF exhibits significantly enhanced tolerance to turbulence-induced spatial distortions compared to the SMF.

The experimental results clearly demonstrate that atmospheric turbulence has a profound impact on fiber-coupled FSO links. While SMF coupling provides stable performance under weak turbulence, it becomes highly susceptible to power fading in strong turbulence due to stringent mode-matching requirements. In contrast, MMF coupling dramatically improves power stability and average received power under identical turbulent conditions. These findings highlight the importance of fiber selection in the design of fiber-converged FSO systems. Although

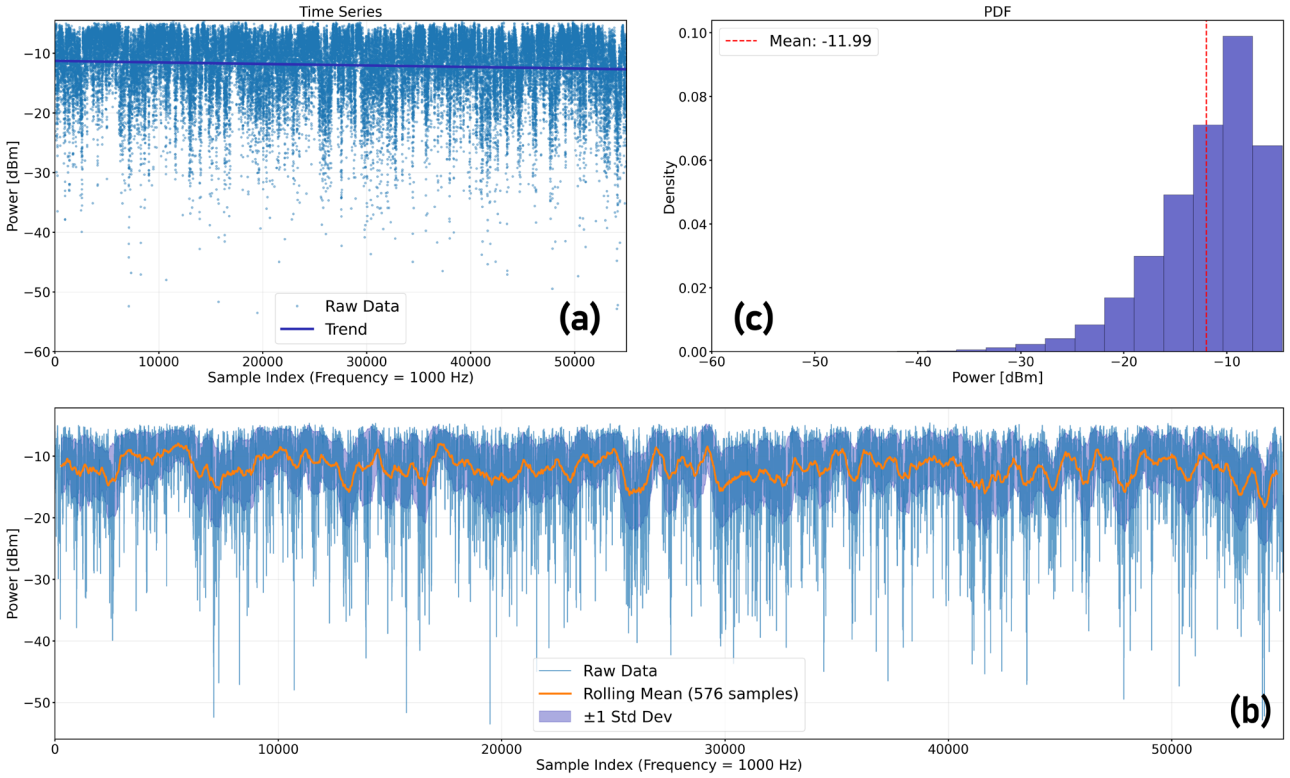

Fig. 6. (a,b) Optical power received (SMF) under strong turbulence conditions with $C_n^2 \approx 10^{-11}$ m$^{-2/3}$; (c) PDF of the measured data as a function of the power.

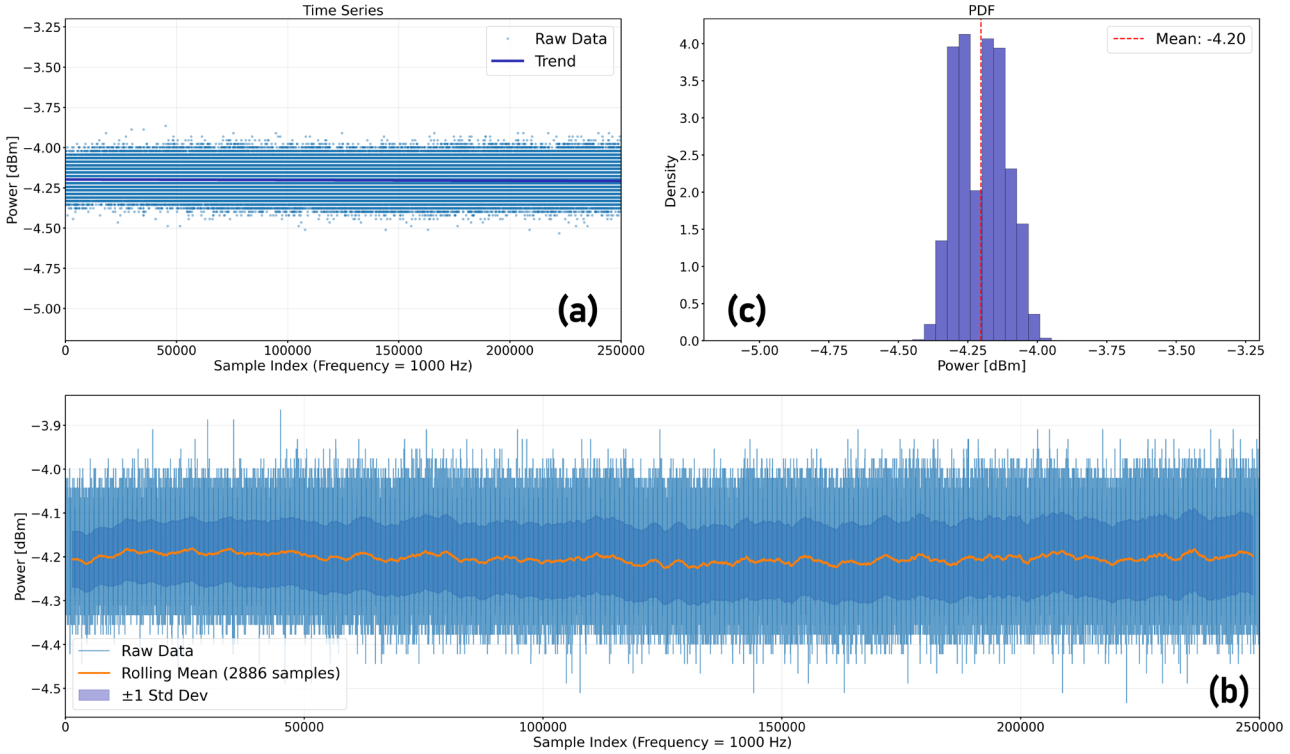

Fig. 7. (a,b) Optical power received (MMF) under strong turbulence conditions with $C_n^2 \approx 10^{-11}$ m$^{-2/3}$; (c) PDF of the measured data as a function of the power.

Table 1. Comparison of power fluctuation metrics for SMF and MMF at different C_n^2.

Fiber type	Refractive index structure parameter C_n^2, $m^{-2/3}$	Mean power, dBm	Standard deviation, dB	Dynamic range, dB
SMF	10^{-16}	–5.01	0.045	0.40
	10^{-11}	–11.99	5.160	48.8
MMF	10^{-11}	–4.19	0.084	0.67

MMF coupling may introduce additional impairments such as modal dispersion, its substantial resilience to turbulence-induced fading makes it a compelling solution for short-reach or receiver-side integration in turbulent environments. More broadly, the results validate the use of controlled atmospheric chambers as effective platforms for systematic evaluation of turbulence effects and fiber-coupling strategies in FSO communication systems.

4. CONCLUSION

This work experimentally investigated the impact of atmospheric turbulence on fiber-converged free-space optical links using a custom-made atmospheric chamber. The chamber enables controlled and repeatable emulation of different turbulence regimes through direct temperature field measurements and real-time estimation of the refractive-index structure parameter C_n^2. Table 1 summarizes measured power statistics for both fiber types under different turbulence regimes.

The results demonstrate that while single-mode fiber coupling is highly sensitive to strong turbulence, exhibiting severe power fading and large fluctuations, multimode fiber coupling provides significantly improved power stability and higher average received power under identical conditions. By analyzing turbulence parameters and received optical power statistics, this study establishes a clear link between the controlled environmental conditions and FSO channel performance, validating the atmospheric chamber as an effective platform for systematic evaluation of turbulence effects in fiber-coupled FSO systems.

REFERENCES

[1] A. Trichili, M. Cox, B. Ooi, M.-S. Alouini. Roadmap to free space optics. *Journal of the Optical Society of America B*, 2020, vol. 37, pp. A184–A201.

[2] M. Mansour Abadi, M. Cox, R. Alsaigh, S. Viola, A. Forbes, M. Lavery. A space division multiplexed free-space-optical communication system that can auto-locate and fully self align with a remote transceiver. *Scientific Reports*, 2019, vol. 9, art. no. 19687.

[3] H. Kaushal, G. Kaddoum. Free space optical communication: Challenges and mitigation techniques. *arXiv*, 2015, art. no. arXiv:1506:04836.

[4] F. Honz, B. Schrenk. Large-core optics for simplified short-range FSO links. *arXiv*, 2024, art. no. arXiv:2406.15399.

[5] J. Krimmer, C. Füllner, W. Freude, C. Koos, S. Randel. Statistical analysis of free-space-to-fiber coupling under atmospheric turbulence. In: L. Caspani, A. Tauke-Pedretti, F. Leo, B. Yang (Eds.). *OSA Advanced Photonics Congress 2020*, OSA Technical Digest, Optica Publishing Group, 2020, art. no. NeM4B.3.

[6] S. Arisa, H. Endo, M. Sasaki, Y. Takayama, R. Shimizu, M. Fujiwara. Coupling efficiency of laser beam to multimode fiber for free space optical communication. *Proceedings of SPIE Vol. 10563. International Conference on Space Optics – ICSO 2014*, 2014, art. no. 105630Y.

[7] M. Li, P. Zhang, T. Wang. Evaluation of atmospheric coherent length of free-space optical links by using phase fluctuation. *Optics Express*, 2024, vol. 32, no. 5, pp. 7243–7253.

[8] Z. Pan, Z. Li, Y. Li, G. Huang, F. Zou, L. Pan, M. Lin, F. Li, C. Geng, X. Li. Experimental demonstration of free-space optical communication under 2 km urban atmosphere using adaptive fiber coupling. *Optics Communications*, 2024, vol. 574, art. no. 131151.

УДК 621.391.64

Исследование влияния атмосферной турбулентности на эффективность систем беспроводной оптической связи с оптоволоконным интерфейсом

Д.Ю. Баловнев, Д.С. Ширяев, И.С. Полухин, Е.С. Колодезный

Институт перспективных систем передачи данных, Университет ИТМО, Биржевая линия, 14, Санкт-Петербург, 199034, Россия

Аннотация. Системы беспроводной оптической связи с оптоволоконным интерфейсом обеспечивают совместимость с современными волоконно-оптическими компонентами: трансиверами и оптоволоконными усилителями. Однако их эффективность в значительной степени определяется качеством ввода принимаемого оптического пучка в одномодовое (SMF) или многомодовое (MMF) оптическое волокно. В данной работе представлена разработанная атмосферная камера, позволяющая осуществлять контролируемое и воспроизводимое моделирование турбулентности с оценкой параметра структуры показателя преломления C_n^2 в реальном времени. С использованием систем беспроводной оптической связи были измерены флуктуации принимаемой оптической мощности для SMF и MMF при одинаковых условиях турбулентности в диапазоне $C_n^2 \approx 10^{-16} - 10^{-11}$ м$^{-2/3}$. Экспериментальные результаты показывают, что сильная турбулентность приводит к значительным флуктуациям мощности при использовании SMF (среднеквадратическое отклонение ≈ 5.16 дБ), тогда как при использовании MMF принимаемая мощность является более стабильной (среднеквадратическое отклонение ≈ 0.08 дБ). Полученные результаты демонстрируют возможность контролируемого и воспроизводимого исследования влияния атмосферных факторов и могут быть использованы при анализе и проектировании подобных систем.

Ключевые слова: беспроводная оптическая связь; атмосферная турбулентность; ввод излучения в оптоволокно